Tetrahedron 66 (2010) 9925–9932

Contents lists available at ScienceDirect

Tetrahedron

journal homepage: www.elsevier.com/locate/tet

Thiazole sulfonamide based ratiometric fluorescent chemosensor with a large spectral shift for zinc sensing

Aasif Helal, Sang Hyun Kim, Hong-Seok Kim *

Department of Applied Chemistry, Kyungpook National University, Daegu 702-701, Republic of Korea

ARTICLE INFO

Article history:
Received 25 September 2010
Received in revised form 19 October 2010
Accepted 20 October 2010
Available online 26 October 2010

Keywords:
Thiazole sulfonamide
Chemosensor
Fluorescence
Ratiometric sensing of Zn^{2+}
ESIPT

ABSTRACT

A new thiazole sulfonamide (TTP, **1**) based Zn^{2+} selective intrinsic chemosensor has been synthesized and investigated. The chemosensor shows a selective fluorescence enhancement (3.0 fold) with Zn^{2+} over biologically relevant cations (Ca^{2+}, Mg^{2+}, Na^{+}, and K^{+}) and biologically non-relevant cations (Cd^{2+}) in an aqueous ethanol system. It produces an increase in the quantum yield and a longer emission wavelength shift (64 nm) on Zn^{2+} binding with the potential of a ratiometric assay.

© 2010 Elsevier Ltd. All rights reserved.

1. Introduction

Fluorescent sensor molecules for the detection of metal ions have attracted considerable research interest and have led to the development of highly specific probes with a broad range of applications in environmental chemistry, biochemistry, and cell biology.[1] Fluorescence-based probes provide high sensitivity and are particularly well suited for the visualization of in vitro and in vivo biologically important metal ions.[2] An ideal fluorescent chemosensor must have a binding-selectivity, i.e., strong affinity for the target molecule and a good signal-selectivity. However, the majority of these chemosensors are based on a mechanism in which the fluorescent output is quenched in the absence of and restored upon binding of the analyte. Nevertheless, the emission intensity depends both on the analyte and on the probe concentrations, which, in a cellular environment, depends on many factors, such as the localization of the probe, membrane permeability, incubation time, and temperature or variations in the cell size. This problem can be solved by using a fluorophore that displays a shift in the peak excitation or emission wavelength upon binding of the analyte. The ratio of the luminescence intensities at two excitation wavelengths are sufficient to determine the analyte concentration, independent of sensor concentration or any instrument-related parameters.[3] Due to the simplicity, high sensitivity, and greater precision of fluorescence assays several such ratiometric probes have been developed for intracellular applications at present.[4]

Among a series of biologically important metal ions, zinc has attracted considerable attention because of its structural significance and catalytic functions with metalloproteins.[5] Although these Zn^{2+} are often tightly bound, chelatable (weakly bound), or free Zn^{2+} also exist in several tissues, including brain tissue,[6] pancreatic tissue,[7] and seminal plasma.[8] The estimation of free zinc has proved to be difficult with classical methods. Moreover, Zn^{2+} is invisible to most analytical techniques due to its spectroscopically silent nature, so fluorescence techniques stand out as the method of choice. A variety of Zn^{2+} selective fluorescent probes that are based on quinoline,[9] fluorescein,[10] indole,[11] and proteins[12] have been developed. But these sensors sometimes show similar affinities for most of the transition and heavy metals, and also lack the suitable ratiometric nature, or if ratiometric, then produce small shifts in the fluorescence wavelength.[13,14] Moreover an emission ratiometric probe is required for imaging using two-photon excitation fluorescence microscopy, which provides significant advantages over standard laser confocal approaches.[15] Several chemosensors based on CHEF (chelation-enhanced fluorescence), ICT (intramolecular charge transfer) or a combination of PET (photoinduced electron transfer), and ICT mechanisms have been designed to produce ratiometric changes on Zn^{2+} binding. These include di-2-picolylamine (DPA) based receptors, such as Zinbo-5,[16a] ZnIC,[16b,c] tosylamido quinoline-based chemosensors, such as TSQ,[16d] Zinquin,[16e] and Schiff-base based receptors like BPBA,[16f] 1,1′-disubstituted ferrocene.[16g] Among these, some of the DPA

* Corresponding author. Tel.: +82 53 950 5588; fax: +82 53 950 6594; e-mail address: kimhs@knu.ac.kr (H.-S. Kim).

0040-4020/$ – see front matter © 2010 Elsevier Ltd. All rights reserved.
doi:10.1016/j.tet.2010.10.055

receptors involve a long synthetic procedure, small emission shift, lack of selectivity, and low quantum yield. Tosylamido quinoline-based chemosensors lack selectivity and form complexes with many metal ions with varying fluorescence intensities, while some Schiff-base receptors have poor solubility and instability in aqueous solutions.

To develop a zinc-selective ratiometric emission probe, the photophysics in cation-induced inhibition of excited-state intramolecular proton transfer (ESIPT) is often used.[17] Recently we have reported some thiazole-based chemosensors in which the thiazole ring is substituted with a phenol at position 2 and a pyridine, phenyl, or another thiazole phenol moiety at position 4 for its use as a ratiometric fluorescence sensor of zinc,[18a] anions,[18b] or the dual chemosensing of zinc and copper,[18c] respectively. The thiazole sulfonamide moiety containing an intramolecular hydrogen bond undergoes ESIPT and yields a highly Stokes shifted emission from the proton-transfer tautomer. Coordination of a metal cation will remove this proton and disrupt the ESIPT process with the emission of the coordinated species occurring with the normal Stokes shift.[19] Moreover introduction of a sulfonamide in the place of a hydroxyl group induces a rapid rate of ESIPT with a high quantum yield of tautomer emission within a wide range of solvents.[17c,19d]

In this paper, the design and development of a novel thiazole sulfonamide-based ratiometric intrinsic fluorescent chemosensor, with substitutions at position 2 and 4 of the thiazole ring, regarding zinc cation in aqueous media is reported. It exhibits a ratiometric fluorescent response upon the addition of Zn^{2+} in 10% water–ethanol, buffered at pH 7.4. The photophysical properties of the sensor on binding with Zn^{2+}, the crucial role of the sulfonamide and the pyridine in the zinc binding, and competitive binding of Zn^{2+} with other metal ions are investigated.

2. Results and discussion

A common fluorophore, such as the amino-benzazoles are often used to develop ESIPT-based zinc chemosensors. The C=N of the thiazole ring is analogous to Schiff-base receptors that has a strong affinity for Zn^{2+}. The combination of sulfonamide and the thiazole ring can act as a binding, as well as a fluorophore, resulting in an intrinsic chemosensor. In order to achieve high fluorescence intensity, selectivity, and affinity for Zn^{2+} detection, instead of a DPA unit, we introduced a 2-pyridyl group at position 4 by a simple synthetic procedure and protected the free amine of the 2-aminophenyl group as a tosylamide, as shown in Fig. 1. To gain insight into the complexation mode of TTP (**1**) for Zn^{2+} we also prepared analogs

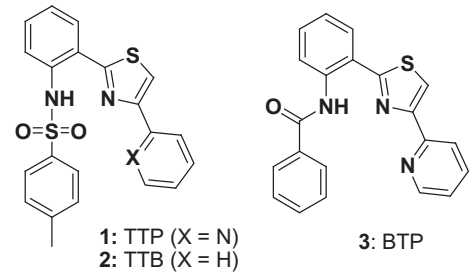

Fig. 1. Structures of chemosensors.

TTB (**2**) and BTP (**3**) (Fig. 1). Sensors **1**, **2**, and **3** were prepared in good yields by the reaction of 2-nitrothiobenzamide with 2-(2-bromoacetyl)pyridine and 2-bromoacetophenone in refluxing ethanol, followed by the reduction of the nitro group to amine and then reaction of the amine with tosyl chloride or benzoyl chloride, as shown in Scheme 1. The structures of **1**, **2**, and **3** were confirmed by ^{1}H NMR, ^{13}C NMR, and elemental analysis. The NMR spectrum of **1**, **2**, and **3** exhibited singlet protons at δ 8.18, δ 7.34, and δ 8.02, respectively, assigned to thiazolyl-*H*, with the NH protons occurring far downfield. In the case of **1** and **3** doublet protons at δ 8.65 and δ 8.52, respectively, were assigned to the pyridyl-*H* nearest to the nitrogen. (Figs. S9–12).

The metal-binding behaviors of TTP (**1**) were determined by UV–vis and fluorescence spectroscopic studies. In order to achieve a physiologically acceptable condition the photophysical properties of TTP (**1**) were examined in a water–ethanol system (1:9). The UV–vis study was carried out in a 10% (v/v) water–ethanol solution buffered by 10 mM HEPES at pH 7.4 with a concentration level of 20 μM. Sensor **1** exhibits a maximal absorption band centered at 289 nm with a shoulder band at 326 nm (Fig. 2). This can be attributed to a π–π^* transition; this is favored by the planar orientation enforced by intramolecular hydrogen bonding.[18,20] When titrated by Zn^{2+} (0–10 equiv), the intensity of the maximal absorption band of TTP (**1**) decreased, with a concomitant increase of the band at 316 nm and the formation of a shoulder band at 373 nm due to the deprotonation of the sulfonamide and disruption of the hydrogen bonding. The absorption bands at 289 and 316 nm linearly decreased and increased, respectively, up to 1 equiv of zinc (Fig. 2 inset), indicating the formation of a 1:1 complex. Free TTP (**1**) in a 10% (v/v) water–ethanol solution buffered by 10 mM HEPES at pH 7.4 with a concentration level of 2 μM exhibits fluorescence with an emission band at 524 nm (Φ_F=0.13, Table 1) with a λ_{ex} at 339 nm (Fig. 3).

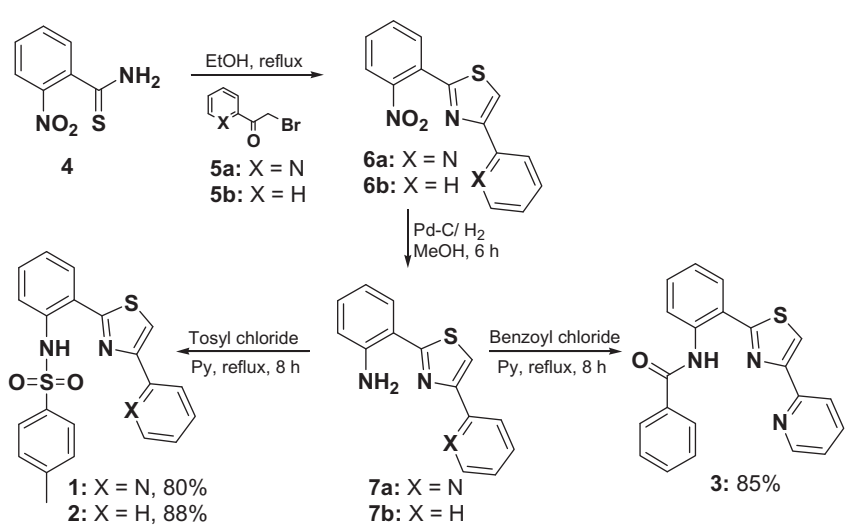

Scheme 1. Preparation of chemosensors TTP (**1**), TTB (**2**), and BTP (**3**).

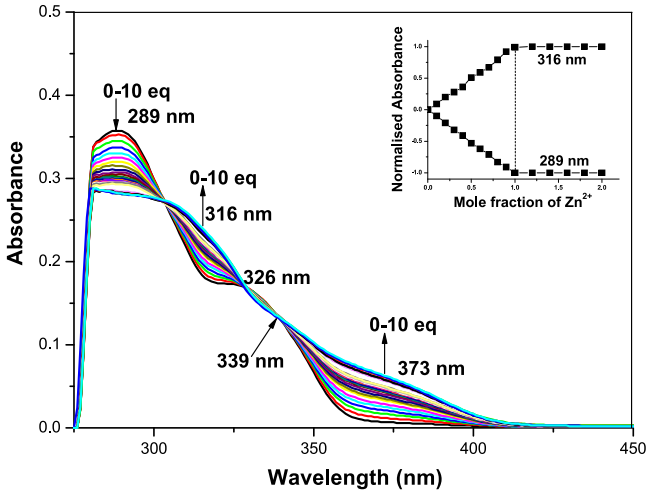

Fig. 2. Changes in UV–vis spectra of **1** (20 μM) upon addition of $Zn(ClO_4)_2$ in H_2O–EtOH (1:9) containing HEPES buffer (10 mM, pH 7.4). Inset: mol ratio plots of absorbance at 289 and 316 nm.

derivatives,[17] TTP (**1**) contains an intramolecular hydrogen bond that undergoes ESIPT and yields a highly Stokes shifted emission from the proton-transfer tautomer (Scheme 2).[19]

This remarkable hypsochromic shift of 64 nm makes TTP (**1**) a potential sensor for Zn^{2+} (Table 1), as compared to DPA, Schiff-base, and Quinoline-based receptors. The fluorescence enhancement was ten times and I/I_0 (fluorescent intensity of receptor $+Zn^{2+}$/fluorescent intensity of receptor) was 3 fold more than our previously reported phenol–thiazole–pyridine receptor.[18a] The Job's plot of TTP (**1**) with Zn^{2+} also indicates the formation of a 1:1 complex (Fig. 4). The binding constant calculated from the fluorescence titration in a water–ethanol system at pH 7.4 was 8.8×10^5 M^{-1} (error limit ≤10%).[21]

In order to study the solvatochromic effect on ESIPT, the binding of Zn^{2+} with **1** was studied in chloroform, ethanol, THF, acetonitrile, and DMSO. The fluorescence property of **1** with Zn^{2+} in all solvents shows similar behavior, i.e., ratiometric increase in fluorescence emissions, except in proton-accepting DMSO, in which **1** produces only normal emission at 454 nm (Table S-1, SI). Since the normal state (enamine, N*) possesses a larger dipole moment than the tautomer state (ketimine, T*) it is selectively stabilized by polar solvents like DMSO and as a result the ESIPT equilibrium is shifted to the normal state, thus increasing its fluorescence intensity.[22] On addition of the Zn^{2+} in DMSO, this normal emission gradually decreases due to chelation-enhanced quenching (CHEQ). The binding

Table 1
Photophysical data and pK_a values of **1**–**3** in H_2O–EtOH (1:9)

Compound	Absorption Max. nm (log ε)		Δλ(nm)	Emission Max. nm		Δλ (nm)	QuantumYield (Φ)[a]		pK_a[b]
	Free	Zn^{2+}		Free	Zn^{2+}		Free	Zn^{2+}	
1	289 (3.95)	316 (3.78)	27	524	460	64	0.13	0.28	11.4
	326 (3.64)	373 (3.20)	47						
2	331 (3.59)	331 (3.59)	0	522	522	0			11.8
3	333 (3.71)	333 (3.71)	0	540	540	0			12.5

[a] Quantum yields were obtained using quinine sulfate in 0.5 M H_2SO_4 as standard.
[b] Calculated from UV–vis absorbance with 20 μM of **1** in H_2O–EtOH (1:9) containing 0.1 M KCl within a pH range 8–13.[17c] (Fig. S-7, SI).

The addition of the Zn^{2+} into **1** gave a new 3.0 fold enhanced emission band centered at 460 nm (Φ_F=0.28, Table 1) with an isoemissive point at 513 nm. The quantum yield of the Zn^{2+} bound species was found to be twice that of some of the DPA (Zinbo-5) and Schiff-base receptors (BPBA). The peaks at 460 and 524 nm showed a linear enhancement and diminution, respectively, with an increase of Zn^{2+} concentration when the ratio of Zn^{2+} and **1** concentration is below or equal to 1:1. When the 1:1 ratio is reached, however, higher Zn^{2+} concentration did not lead to any further emission enhancement (Fig. 3 inset). Like the benzothiazole

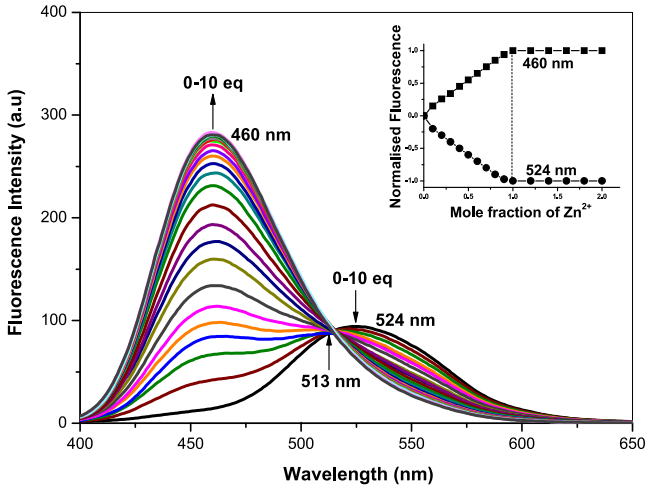

Fig. 3. Changes in fluorescence spectra of **1** (2 μM) in H_2O–EtOH (1:9) containing HEPES buffer (10 mM, pH 7.4), 1.0 mM EGTA and 100 mM KCl with different concentration of free (unbound) Zn^{2+} (0–20 μM) (λ_{ex}=339 nm). Inset: mol ratio plots of emissions at 460 and 524 nm.

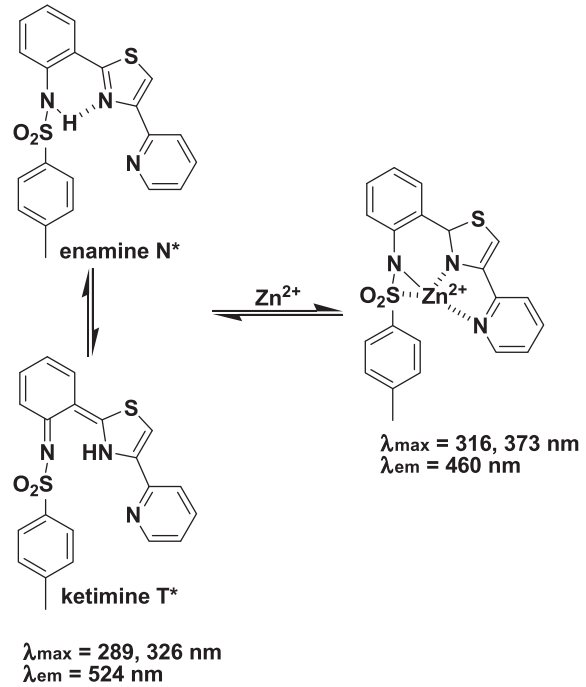

Scheme 2. The possible ESIPT in **1** and binding with Zn^{2+} in a 1:1 binding stoichiometry.

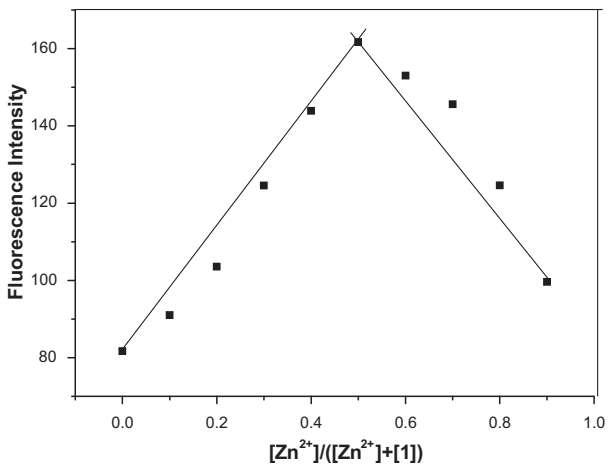

Fig. 4. Fluorescence Job's plot of **1** with $Zn(ClO_4)_2$ in H_2O–EtOH (1:9) containing HEPES buffer (10 mM, pH 7.4), 1.0 mM EGTA and 100 mM KCl measured at 460 nm.

constants were calculated to be 4.3×10^5 M^{-1} in acetonitrile and 7.2×10^5 M^{-1} in DMSO (error limit $\leq$10%) (Fig. S-1 and S-2, SI).

The Zn^{2+} specific ratiometric response of TTP (**1**) was further confirmed by screening with the 10 equiv of biologically relevant metal ions, such as Na^+, K^+, Mg^{2+}, and Ca^{2+}, and non-biologically relevant metal ions, such as Cd^{2+}. As shown in Fig 5 only Zn^{2+} among the all tested metal ions induced a distinct emission shift and enhancement. The paramagnetic transition-metal ions Fe^{2+}, Fe^{3+}, and Cu^{2+} coordinate to TTP (**1**), but partially or completely quench the fluorescence emission. Successful emission color change on Zn^{2+} binding is easily observable by a naked eye examination of the receptor **1**, with different cations. Upon excitation at 365 nm the green fluorescence of **1** changes to blue fluorescence, only in the case of Zn^{2+} as compared to other metal ions (Fig. 6).

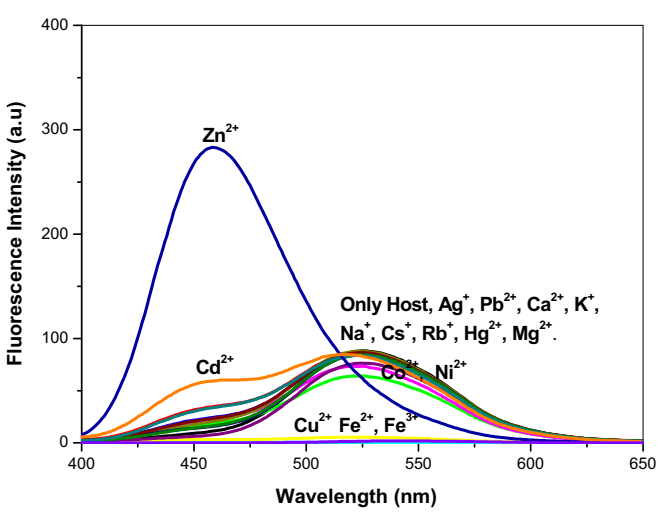

Fig. 5. Fluorescence spectra of **1** (2 μM) in H_2O–EtOH (1:9) containing HEPES buffer (10 mM, pH 7.4), 1.0 mM EGTA and 100 mM KCl upon addition of various metal ions (10 equiv) with an excitation wavelength of 339 nm.

The quenching in the case of Fe^{2+}, Fe^{3+}, and Cu^{2+} is due to the very fast and efficient non-radiative decay of the excited states, due to the electron or energy transfer between the open shell d-orbitals of the metal ions and TTP (**1**).[23] While Zn^{2+}, has the closed-shell d-orbitals, so that energy or electron transfer processes cannot take place. Coordination of Zn^{2+} removes the sulfonamide proton and disrupts ESIPT, thus causing emission with a normal Stokes shift.[17,24]

Moreover in a competitive binding experiment the presence of Na^+, K^+, Mg^{2+}, and Ca^{2+}, which are abundant in cells, did not interfere with the ratiometric response to Zn^{2+}, even though their concentrations were 100 times higher than Zn^{2+} concentration as illustrated in Fig S-3 (SI). Except in the cases of Fe^{2+}, Fe^{3+}, and Cu^{2+}, where the enhancement was smaller when compared to the others. Also the ratiometric response of **1** for Zn^{2+} was found to be maximum as compared to other cations (Fig. 7); thus, TTP selectivity for Zn^{2+} detection over other heavy metals and Cd^{2+} was found to be better than some Schiff-base and DPA receptors in aqueous ethanol.

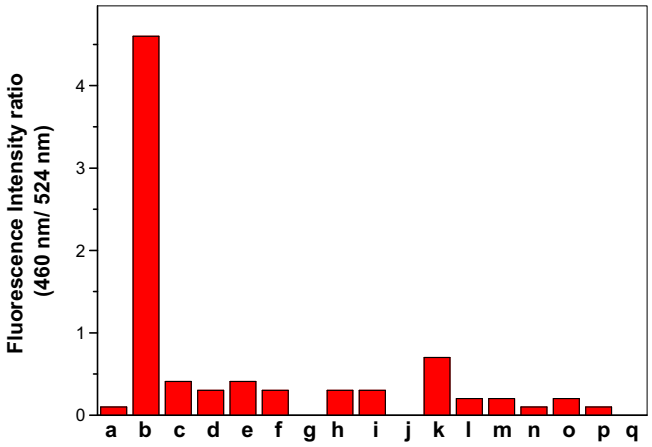

Fig. 7. Enhancement of fluorescence intensity of **1** (2 μM) in H_2O–EtOH (1:9) containing HEPES buffer (10 mM, pH 7.4), 1.0 mM EGTA and 100 mM KCl by addition of 10 equiv of respective metal ion. (a) **1** only, (b) **1**+Zn^{2+}, (c) **1**+Ag^+, (d) **1**+Hg^{2+}, (e) **1**+Pb^{2+}, (f) **1**+Ca^{2+}, (g) **1**+Cu^{2+}, (h) **1**+Ni^{2+}, (i) **1**+Co^{2+}, (j) **1**+Fe^{2+}, (k) **1**+Cd^{2+}, (l) **1**+Mg^{2+}, (m) **1**+K^+, (n) **1**+Na^+, (o) **1**+Cs^+, (p) **1**+Rb^+, (q) **1**+Fe^{3+}.

The detection limit of **1** for Zn^{2+} was found to be 0.2 μM, which is sufficient for sensing Zn^{2+} in the biological system (Fig. S-4, SI).[25] All of these facts indicate that this probe can be employed for a wide range of biological applications using microscopic techniques.

Due to the spectroscopically and magnetically silent nature of zinc, it was not possible to examine its ground state behavior in an ethanol–water system (Fig. S-5, SI).[26] However, the ground state behavior of the zinc complexation and ion recognition was evaluated in DMSO-d_6. A partial ^1H NMR spectrum of TTP (**1**), upon addition of 1 equiv of Zn^{2+} is shown in Fig 8. Upon addition of 1 equiv of Zn^{2+} the N–H proton peak disappeared due to deprotonation and the signals of H_a and H_b shifted downfield due to the deshielding effect of the metal ion. However, in the case of protons H_d, H_e, and H_f experienced an upfield shift. It possibly resulted from an aromatic sulfonamide–metal π-*d* orbital interaction through space (Scheme 3).[27]

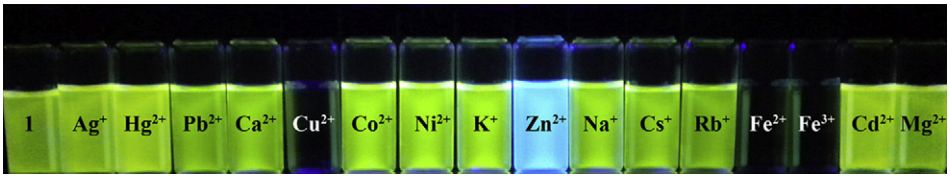

Fig. 6. Fluorogenic change in a 20 μM solution of **1** in H_2O–EtOH (1:9) in the presence of 10 equiv of every cation upon illumination at 365 nm.

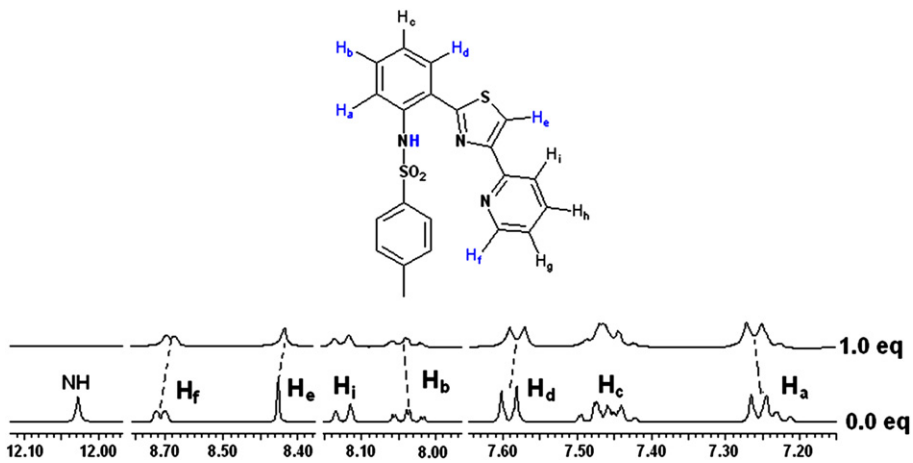

Fig. 8. Partial ^{1}H NMR spectra of **1** with $Zn(ClO_4)_2$ in DMSO-d_6.

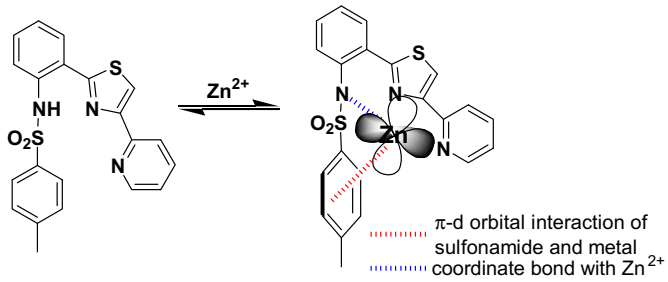

Scheme 3. Chelation of **1** with Zn^{2+} showing the aromatic-metal π-d orbital interaction.

To understand the crucial role of the pyridine unit in position 4 of the thiazole ring, which acts as an additional binding site for the Zn^{2+} with the aid of the sulfonamide, we have synthesized the corresponding phenyl derivative TTB (**2**) bearing the phenyl unit in position 4 of the thiazole ring.[28] Subsequently, it was tested for absorption and fluorescence changes upon addition of the Zn^{2+}. As seen in Figs. 9a and b, unlike TTP (**1**), there are no absorption spectral changes upon addition of Zn^{2+}. In the case of the fluorescence spectrum there is little enhancement of the emission peak in TTB (**2**) on Zn^{2+} addition and there is no ratiometric change (Figs. 9c and d). The binding constant of **2** with Zn^{2+} calculated from the fluorescence titration (Fig. S-6, SI) in a water–ethanol system at pH 7.4 was 1.8×10^5 M^{-1} (error limit $\leq$10%).[21] This strongly suggests that increasing the Zn^{2+} coordination number of the TTB (**2**) by introducing a pyridine at the position 4, not only increases the zinc binding ability but also defines the Zn^{2+} binding mode by making it ratiometric.

Sulfonamides tightly bind only to the zinc holoenzyme and not to the metal-free apoenzyme. This property clearly facilitates the use of sulfonamide fluorophores to measure zinc binding to a carbonic anhydrase II-based biosensor.[29] To gain an insight into the complexation mode of Zn^{2+} and the role of sulfonamide, we prepared BTP (**3**).

In contrast to **1**, BTP (**3**, ——), which has benzamide in the place of sulfonamide did not reveal any significant changes in absorption and fluorescence emission upon addition up to 10 equiv of Zn^{2+} as

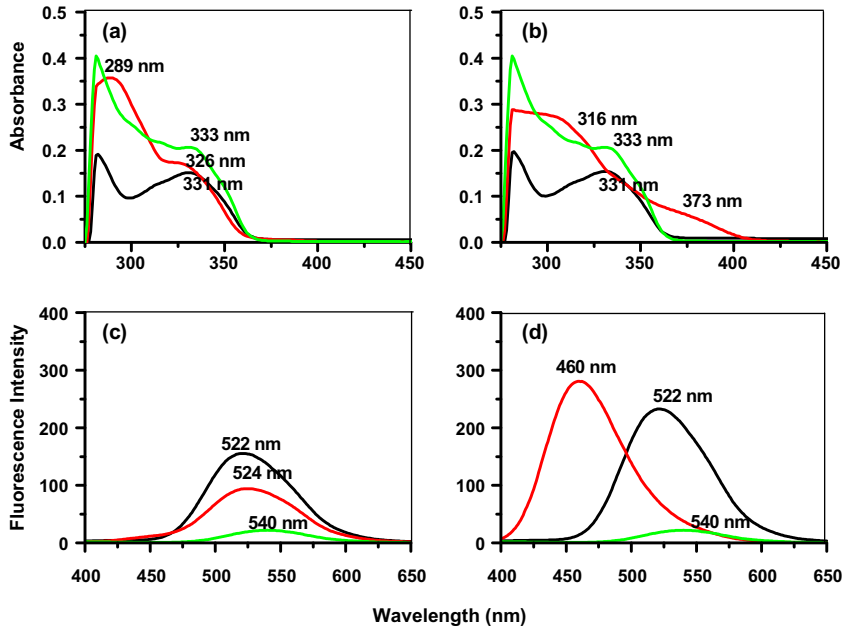

Fig. 9. UV–vis spectra of **1** (——), **2** (——) and **3** (——): (a) in the absence, (b) in the presence of 10 equiv of $Zn(ClO_4)_2$ in H_2O–EtOH (1:9) containing HEPES buffer (10 mM, pH 7.4). Fluorescence spectra of **1** (——), **2** (——) and **3** (——): (c) in the absence and (d) in the presence of 10 equiv of $Zn(ClO_4)_2$ in H_2O–EtOH (1:9) containing HEPES buffer (10 mM, pH 7.4).

shown in Fig. 9. The pK_a value of **3** (pK_a=12.5) was found to be greater than **1** (pK_a=11.4), which makes the N–H proton less acidic and resulting in a very low tautomer emission in **3** than **1** (Table 1, and Fig. 9). Thus, it is notable that the sulfonamide group of **1** plays two important roles in Zn^{2+} complexation: (a) it increases the acidity of the N–H proton (Table 1) leading to a stronger intramolecular hydrogen bonding that results in a rapid rate of ESIPT and quantum yield of the tautomer emission (Φ=0.13), and (b) the sulfonamide N^- anion is a stronger donor[30] than the parent neutral amino, or the benzamide group, so it enhances the fluorescence and forms a stronger stable binding with Zn^{2+} (Φ=0.28).

We prepared the complex of TTP (**1**) with Zn^{2+} in H_2O–EtOH (1:9) and characterized by HR-FAB mass (Fig. S-8, SI). The HR mass spectra of **1**-Zn^{2+} shows a 1:1 stoichiometry with the molecular ion peak at *m*/*z* 469.9975, which can be assigned as the signal for $[M+Zn-H]^+$.

Hartree–Fock 3-21G calculations using Spartan 04 of **1** and its Zn^{2+} complex support our hypothesis that the C=N of the thiazole, nitrogen of the pyridine ring, and the sulfur of the sulfonamide are responsible for Zn^{2+} coordination having a bond length of 1.92 Å, 2.01 Å, and 2.82 Å, respectively. The energy-minimized calculations also revealed that the benzene ring, along with the thiazole, and pyridine rings, are on the same plane as the Zn^{2+} while the tosyl group makes an angle of 95.54° (Fig. 10).

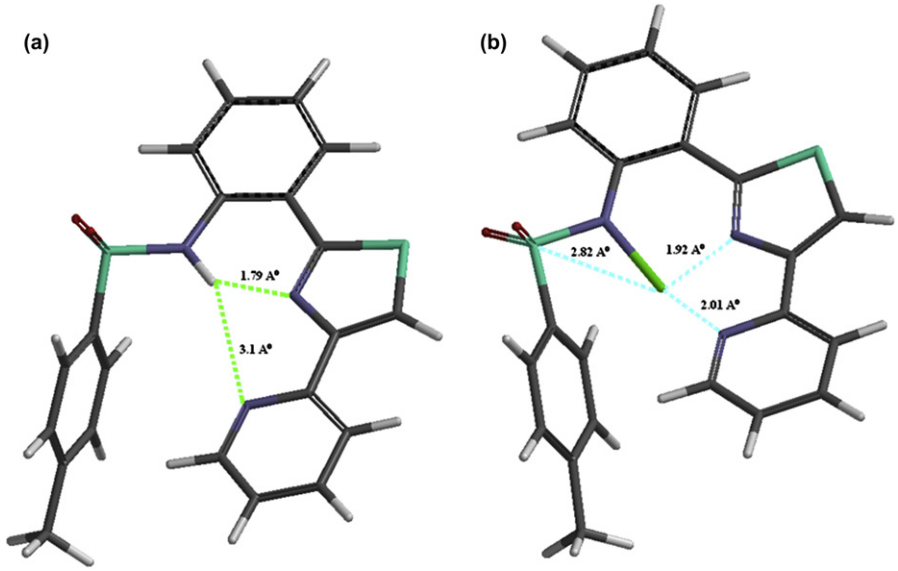

Fig. 10. Energy minimized structures of (a) **1** and (b) **1**–Zn^{2+} complex as predicted by Hartree–Fock 3-21G calculations.

Thus we have prepared an intrinsic fluorescent probe whose fluorescent unit is directly involved in the interaction with metal ions helping in quick, sensitive, and selective detection of Zn^{2+}.

3. Conclusion

In conclusion, we have developed a new sulfonamide–thiazole–pyridine based ratiometric intrinsic fluorescent probe TTP (**1**), highly selective for Zn^{2+} over other biologically relevant, non-relevant, and transitional metal cations on the basis of the ESIPT mechanism. Upon complexation, the Zn^{2+}-bound species exhibits a significantly large blue shift (64 nm), enhancement (3.0 fold) in the emission spectrum, and an increase in the quantum yield, which amplifies the recognition event to a greater extent than other commonly used DPA and Schiff-base receptors, as well as our previously reported phenol–thiazole–pyridine compound. The TTP utilizes the C=N of the thiazole ring, similar to the Schiff-base receptor and the pyridine ring like the DPA receptor, for production of the ratiometric fluorescence signal and strong binding affinity with Zn^{2+} in aqueous ethanol. Thus, the TTP receptor involves simple synthetic procedures, overcomes the poor solubility and instability of the Schiff-base receptors in an aqueous system, lack of selectivity of the tosylamido quinoline receptors, and is suitable for ratiometric imaging of Zn^{2+} in biological system.

4. Experimental section

4.1. General methods

Melting points were determined using a Thomas–Hoover capillary melting point apparatus and are uncorrected. ^{1}H and ^{13}C NMR spectra were recorded on a Bruker AM-400 FT NMR spectrometer using Me_4Si as the internal standard. Mass-spectral data were obtained from the Korea Basic Science Institute (Daegu) on a Jeol JMS 700 High resolution mass spectrometer. UV–vis absorption spectra were determined on a Shimadzu UV-1650PC spectrophotometer. Fluorescence spectra were measured on a Shimadzu RF-5301 fluorescence spectrometer equipped with a xenon discharge lamp and 1 cm quartz cells. All of the measurements were carried out at 298 K.

Absolute ethanol of analytical grade was purchased from Merck. Deionized water (double distilled) was used throughout the experiment as an aqueous layer. All other materials used for synthesis were purchased from Aldrich Chemical Co. and used without further purification. 2-Nitrobenzthioamide (**4**)[31] and 2-(bromoacetyl) pyridine (**5a**),[32] compounds **6b** and **7b**[33] were prepared in accordance with the procedure in the literature. The solutions of metal ions were prepared from their perchlorate salts of analytical grade and then subsequently diluted to prepare working solutions. HEPES buffer solutions of different pH were prepared using proper amount of HEPES and KOH (all of analytical grade) under adjustment by a pH meter. All fluorescence experiments were carried out at pH 7.4 in buffered Zn^{2+} solution comprising of 10 mM HEPES (buffer), 1.0 mM EGTA as Zn^{2+} chelator, and 100 mM KCl in accordance with the procedure reported in the literature.[5b]

4.2. Determination of quantum yields

Quantum yields were determined by the relative comparison procedure.[34] The quinine sulfate with the quantum yield of 0.54 in sulfuric acid (0.5 M) was used as the standard. The general

equation used in the determination of relative quantum yields is shown as follows:

$$Q_x/Q_{st} = (F_x/F_{st}) \times (A_{st}/A_x) \times \left(n_x^2/n_{st}^2\right)$$

Where Q is the quantum yields; F is the integrated area under the corrected emission spectrum; A is the absorbance at the excitation wavelength; n is the refractive index of the solution; and the subscripts x and st refer to the unknown, and the standard, respectively.

4.3. Synthesis

*4.3.1. 2(2′-Nitrophenyl)-4-pyridylthiazole (**6a**).* A mixture of **4** (100 mg, 0.55 mmol) and **5a** (185 mg, 0.66 mmol) in ethanol (15 mL) was refluxed for 4 h. The solvent was removed under vacuo and the residue was washed with water, neutralized with 1 N NaOH, and extracted with EtOAc. The organic layer was dried over anhydrous sodium sulfate and concentrated. The residue was purified using column chromatography (SiO_2, EtOAc–hexane-1:2) to give **6a** (124 mg, 80% yield). Mp: 88°C (CH_2Cl_2 –hexane); ^{1}H NMR (400 MHz, $CDCl_3$) δ 7.51 (dt, J=7.8, 1.5 Hz, 1H), 7.58 (dt, J=7.8, 1.5 Hz, 1H), 7.74–7.70 (m, 3H), 8.01 (d, J=7.8 Hz, 1H), 8.18 (s, 1H), 8.25–8.22 (m, 1H), 8.53 (d, J=4.4 Hz, 1H); ^{13}C NMR (100 MHz, $CDCl_3$) δ 119.0, 121.7, 123.3, 125.6, 126.9, 130.6, 131.1, 132.1, 134.4, 137.5, 149.1, 151.8, 156.1, 161.9. Anal. Calcd for $C_{14}H_9N_3O_2S$: C, 59.35; H, 3.20; N, 14.83; S, 11.32. Found: C, 59.14; H, 3.11; N, 14.79; S, 11.40.

*4.3.2. Chemosensor **1**.* A solution of **6a** (200 mg, 0.70 mmol) in methanol (10 mL) was hydrogenated with 10% Pd/C under 1 atm of hydrogen for 6 h. After the catalyst was removed by filtration the filtrate was concentrated and dried to give the crude amine **7a**. To the solution of the crude amine (**7a**, 120 mg, 0.47 mmol) in pyridine (20 mL) *p*-toluenesulfonyl chloride (112 mg, 0.59 mmol) was added and refluxed for 8 h. The mixture was diluted with water and extracted with EtOAc. The organic layer was dried over anhydrous sodium sulfate and concentrated. The residue was purified by column chromatography (SiO_2, EtOAc–hexane-1:2) to give **1** (154 mg, 80% yield). Mp: 165°C (CH_2Cl_2–hexane); ^{1}H NMR (400 MHz, $CDCl_3$) δ 2.27 (s, 3H, CH_3), 7.08 (d, J=8.3 Hz, 3H), 7.32 (t, J=7.8 Hz, 2H), 7.61 (d, J=8.3 Hz, 2H), 7.64 (d, J=8.3 Hz, 1H), 7.72 (d, J=8.3 Hz, 1H), 7.91 (dt, J=7.7, 1.3 Hz, 1H), 8.13 (s, 1H), 8.23 (d, J=7.8 Hz, 1H), 8.65 (d, J=4.4 Hz, 1H), 12.33 (s, 1H, NH); ^{13}C NMR (100 MHz, $CDCl_3$) δ 21.5, 116.6, 120.1, 120.2, 121.1, 123.5, 123.8, 127.2, 128.7, 129.5, 131.2, 136.1, 136.4, 138.0, 143.7, 149.5, 151.2, 154.7, 168.0. Anal. Calcd for $C_{21}H_{17}N_3O_2S_2$: C, 61.89; H, 4.20; N, 10.31; S, 15.74. Found: C, 61.75; H, 4.24; N, 10.25; S, 15.67.

*4.3.3. Chemosensor **2**.* To the solution of the crude amine **7b** (120 mg, 0.48 mmol) in pyridine (20 mL) *p*-toluenesulfonyl chloride (112 mg, 0.59 mmol) was added and refluxed for 8 h. The mixture was diluted with water and extracted with EtOAc. The organic layer was dried over anhydrous sodium sulfate and concentrated. The residue was purified by column chromatography (SiO_2, EtOAc–hexane-1:9) to give **2** (172 mg, 88% yield). Mp: 144–145°C (CH_2Cl_2–hexane); ^{1}H NMR (400 MHz, $CDCl_3$) δ 2.17 (s, 3H, CH_3), 6.95 (m, 3H), 7.21 (t, J=8.0 Hz, 1H), 7.29 (t, J=7.2 Hz, 1H), 7.34 (s, 1H), 7.41 (t, J=7.6 Hz, 2H), 7.55–7.50 (m, 3H), 7.64 (d, J=8.8 Hz, 1H), 7.88 (d, J=8.0 Hz, 2H), 12.35 (s, 1H, NH); ^{13}C NMR (100 MHz, $CDCl_3$) δ 21.5, 112.1, 120.1, 120.3, 123.7, 126.2, 127.2, 128.7, 128.8, 129.3, 129.5, 131.0, 133.1, 136.1, 136.5, 143.6, 155.0, 167.8. Anal. Calcd for $C_{22}H_{18}N_2O_2S_2$: C, 65.00; H, 4.46; N, 6.89; S, 15.78. Found: C, 64.84; H, 4.36; N, 6.87; S, 15.58.

*4.3.4. Chemosensor **3**.* To the solution of the crude amine **7a** (120 mg, 0.47 mmol) in pyridine (20 mL) benzoyl chloride (80 mg, 0.56 mmol) was added and refluxed for 8 h. The mixture was diluted with water and extracted with EtOAc. The organic layer was dried over anhydrous sodium sulfate and concentrated. The residue was purified by column chromatography (SiO_2, EtOAc–hexane-1:4) to give **3** (143 mg, 85% yield). Mp: 104–105°C (CH_2Cl_2 –hexane); ^{1}H NMR (400 MHz, $CDCl_3$) δ 7.06 (t, J=7.3 Hz, 1H), 7.16 (dt, J=5.3, 1.8 Hz, 1H), 7.29 (t, J=7.8 Hz, 2H), 7.38 (t, J=7.3 Hz, 1H), 7.46 (q, J=7.3 Hz, 2H), 7.59 (d, J=7.8 Hz, 1H), 7.71 (d, J=6.8 Hz, 1H), 7.90 (d, J=7.4 Hz, 2H), 8.02 (s, 1H), 8.52 (d, J=4.3 Hz, 1H), 8.84 (d, J=8.6 Hz, 1H), 12.54 (s, 1H, NH); ^{13}C NMR (100 MHz, $CDCl_3$) δ 117.1, 119.8, 121.2, 121.4, 123.2, 123.5, 127.9, 128.7, 128.9, 131.4, 131.7, 135.9, 137.1, 137.2, 149.4, 151.3, 155.0, 166.7, 169.2. Anal. Calcd for $C_{21}H_{15}N_3OS \cdot CH_2Cl_2$: C, 59.73; H, 3.87; N, 9.50; S, 7.25. Found: C, 60.10; H, 3.94; N, 9.53; S, 6.99.

*4.3.5. Zn^{2+}–**1** complex.* A mixture of **1** (100 mg, 0.24 mmol) and Zn $(ClO_4)_2 \cdot 6H_2O$ (110 mg, 0.29 mmol) in ethanol–water (v/v 9:1, 5 mL) was refluxed for 3 h. The mixture was cooled to room temperature and the precipitated complex was filtered off. The filtered cake was washed thoroughly with water, ethanol, and diethyl ether, and dried under vacuum to provide the complex (85 mg, 74% yield). HR-FAB mass: calcd for ($C_{21}H_{16}O_2N_3S_2Zn$) 469.9975. Found: 469.9972.

Acknowledgements

This research was supported by the Basic Science Research Program through the National Research Foundation of Korea (NRF), and funded by the Ministry of Education, Science and Technology (20100010070). A.H. was also supported by the Research Institute of Industrial Technology at Kyungpook National University.

Supplementary data

Supplementary data related to this article can be found online version at doi:10.1016/j.tet.2010.10.055.

References and notes

1. deSilva, A. P.; Gunaratne, H. Q. N.; Gunnlaugsson, T.; Huxley, A. J. M.; McCoy, C. P.; Rademacher, J. T.; Rice, T. E. *Chem. Rev.* **1997**, *97*, 1515.
2. Mason, W. T. *Fluorescent and Luminescent Probes for Biological Activity*; Academic: San Diego, 1999.
3. Grynkiewicz, G.; Poenie, M.; Tsien, R. Y. *J. Biol. Chem.* **1985**, *260*, 3440.
4. (a) Haugland, R. P. *Handbook of Fluorescent Probes and Research Chemicals*; Molecular Probes: Eugene, 1996; (b) Hirano, T.; Kikuchi, K.; Urano, Y.; Nagano, T. *J. Am. Chem. Soc.* **2002**, *124*, 6555; (c) Mizukami, S.; Okada, S.; Kimura, S.; Kikuchi, K. *Inorg. Chem.* **2009**, *48*, 7630; (d) Komatsu, T.; Urano, Y.; Fujikawa, Y.; Kobayashi, T.; Kojima, H.; Terai, T.; Hanaoka, K.; Nagano, T. *Chem. Commun.* **2009**, 7015; (e) Zhang, X.; Hayes, D.; Smith, S. J.; Friedle, S.; Lippard, S. J. *J. Am. Chem. Soc.* **2008**, *130*, 15788; (f) Nolan, E. M.; Lippard, S. J. *Acc. Chem. Res.* **2009**, *42*, 193.
5. (a) Lippard, S. J.; Berg, J. M. *Principles of Bioinorganic Chemistry*; University Science Books: Mill Valley, 1994; (b) Sensi, S. L.; Canzoniero, L. M. T.; Yu, S. P.; Ying, H. S.; Koh, J. Y.; Kerchner, G. A.; Choi, D. W. *J. Neurosci.* **1997**, *17*, 9554; (c) Coleman, J. E. *Curr. Opin. Chem. Biol.* **1998**, *2*, 222; (d) Kikuchi, K. *Chem. Soc. Rev.* **2010**, *39*, 2048.
6. (a) Frederickson, C. J. *Int. Rev. Neurobiol.* **1989**, *31*, 145; (b) Frederickson, C. J.; Koh, J. Y.; Bush, A. I. *Nat. Rev. Neurosci.* **2005**, *6*, 449.
7. Gyulkhandanyan, A. V.; Lu, H. F.; Lee, S. C.; Bhattacharjee, A.; Wijesekara, N.; Fox, J. E. M.; MacDonald, P. E.; Chimienti, F.; Dai, F. F.; Wheeler, M. B. *J. Biol. Chem.* **2008**, *283*, 10184.
8. Edstrom, A. M. L.; Malm, J.; Frohm, B.; Martellini, J. A.; Giwercman, A.; Morgelin, M.; Cole, A. M.; Sorensen, O. E. *J. Immunol.* **2008**, *181*, 3413.
9. (a) Zalewski, P. D.; Forbes, I. J.; Betts, W. H. *Biochem. J.* **1993**, *296*, 403; (b) Mikata, Y.; Yamanaka, A.; Yamashita, A.; Yano, S. *Inorg. Chem.* **2008**, *47*, 7295.
10. (a) Burdette, S. C.; Walkup, G. K.; Spingler, B.; Tsien, R. Y.; Lippard, S. J. *J. Am. Chem. Soc.* **2001**, *123*, 7831; (b) Gee, K. R.; Zhou, Z. L.; Qian, W. J.; Kennedy, R. *J. Am. Chem. Soc.* **2002**, *124*, 776.
11. Taki, M.; Watanabe, Y.; Yukio, Y. *Tetrahedron Lett.* **2009**, *50*, 1345.
12. (a) Van Dongen, E.; Dekkers, L. M.; Spijker, K.; Meijer, E. W.; Klomp, L. W. J.; Merkx, M. *J. Am. Chem. Soc.* **2006**, *128*, 10754; (b) Bozym, R. A.; Thompson, R. B.; Stoddard, A. K.; Fierke, C. A. *ACS Chem. Biol.* **2006**, *1*, 103; (c) Evers, T. H.; Appelhof, M. A. M.; de Graaf-Heuvelmans, P.; Meijer, E. W.; Merkx, M. *J. Mol. Biol.* **2007**, *374*, 411; (d) Evers, T. H.; Appelhof, M. A. M.; Meijer, E. W.; Merkx, M.

Protein Eng., Des. Sel. **2008**, *21*, 529; (e) Vinkenborg, J. L.; Nicolson, T. J.; Bellomo, E. A.; Koay, M. S.; Rutter, G. A.; Merkx, M. *Nat. Methods* **2009**, *6*, 737.
13. (a) Jiang, P. J.; Guo, Z. J. *Coord. Chem. Rev.* **2004**, *248*, 205; (b) Kikuchi, K.; Komatsu, K.; Nagano, T. *Curr. Opin. Chem. Biol.* **2004**, *8*, 182; (c) Carol, P.; Sreejith, S.; Ajayaghosh, A. *Chem. Asian J.* **2007**, *2*, 338.
14. (a) Gee, K. R.; Zhou, Z. L.; Ton-That, D.; Sensi, S. L.; Weiss, J. H. *Cell Calcium* **2002**, *31*, 245; (b) Maruyama, S.; Kikuchi, K.; Hirano, T.; Urano, Y.; Nagano, T. *J. Am. Chem. Soc.* **2002**, *124*, 10650; (c) Woodroofe, C. C.; Lippard, S. J. *J. Am. Chem. Soc.* **2003**, *125*, 11458; (d) Chang, C. J.; Jaworski, J.; Nolan, E. M.; Sheng, M.; Lippard, S. J. *Proc. Natl. Acad. Sci. U.S.A.* **2004**, *101*, 1129; (e) Ajayaghosh, A.; Carol, P.; Sreejith, S. *J. Am. Chem. Soc.* **2005**, *127*, 14962; (f) Kiyose, K.; Kojima, H.; Urano, Y.; Nagano, T. *J. Am. Chem. Soc.* **2006**, *128*, 6548; (g) Bredas, J. L.; Perry, J. W.; Fahrni, C. J. *J. Am. Chem. Soc.* **2007**, *129*, 11888; (h) Sreejith, S.; Divya, K. P.; Ajayaghosh, A. *Chem. Commun.* **2008**, 2903; (i) Li, Z. F.; Xiang, Y.; Tong, A. *Anal. Chim. Acta* **2008**, *619*, 75.
15. Potter, S. M.; Wang, C. M.; Garrity, P. A.; Fraser, S. E. *Gene* **1996**, *173*, 25.
16. (a) Taki, M.; Wolford, J. L.; O'Halloran, T. V. *J. Am. Chem. Soc.* **2004**, *126*, 712; (b) Komatsu, K.; Urano, Y.; Kojima, H.; Nagano, T. *J. Am. Chem. Soc.* **2007**, *129*, 13447; (c) Hanaoka, K.; Muramatsu, Y.; Urano, Y.; Terai, T.; Nagano, T. *Chem. Eur. J.* **2010**, *16*, 568; (d) Frederickson, C. J.; Kasarskis, E. J.; Ringo, D.; Frederickson, R. E. *J. Neurosci. Methods* **1987**, *20*, 91; (e) Zhang, Y.; Guo, X.; Si, W.; Jia, L.; Qian, X. *Org. Lett.* **2008**, *10*, 473; (f) Wu, Z.; Zhang, Y.; Ma, J. S.; Yang, G. *Inorg. Chem.* **2006**, *45*, 3140; (g) Zapata, F.; Caballero, A.; Espinosa, A.; Tarraga, A.; Molina, P. *Org. Lett.* **2007**, *9*, 2385.
17. (a) Henary, M. M.; Fahrni, C. J. *J. Phys. Chem. A* **2002**, *106*, 5210; (b) Henary, M. M.; Wu, Y. G.; Fahrni, C. J. *Chem. Eur. J.* **2004**, *10*, 3015; (c) Henary, M. M.; Wu, Y.; Cody, J.; Sumalekshmy, S.; Li, J.; Mandal, S.; Fahrni, C. J. *J. Org. Chem.* **2007**, *72*, 4784.
18. (a) Helal, A.; Kim, H.-S. *Tetrahedron Lett.* **2009**, *50*, 5510; (b) Helal, A.; Thao, N. T. T.; Lee, S.; Kim, H.-S. *J. Inclusion Phenom. Macrocyclic Chem.* **2010**, *66*, 87; (c) Helal, A.; Lee, S. H.; Kim, S. H.; Kim, H.-S. *Tetrahedron Lett.* **2010**, *51*, 3531.
19. (a) Das, K.; Sarkar, N.; Majumdar, D.; Bhattacharyya, K. *Chem. Phys. Lett.* **1992**, *198*, 443; (b) Sinha, H. K.; Dogra, S. K. *Chem. Phys.* **1986**, *102*, 337; (c) Mosquera, M.; Penedo, J. C.; Rios Rodriguez, M. C.; Rodriguez-Prieto, F. *J. Phys. Chem.* **1996**, *100*, 5398; (d) Santra, S.; Krishnamoorthy, G.; Dogra, S. K. *J. Phys. Chem. A* **2000**, *104*, 476; (e) Santra, S.; Dogra, S. K. *Chem. Phys.* **1998**, *226*, 285.
20. Keck, J.; Kramer, H. E. A.; Port, H.; Hirsch, T.; Fischer, P.; Rytz, G. *J. Phys. Chem.* **1996**, *100*, 14468.
21. (a) Connors, K. A. *Binding Constants: The Measurement of Molecular Complex Stability*; Wiley: New York, NY, 1987; pp 21–101; 339–343; (b) Forgues, S. F.; LeBris, M. T.; Gutte, J. P.; Valuer, B. *J. Phys. Chem.* **1988**, *92*, 6233.
22. (a) Klymchenko, A. S.; Demchenko, A. P. *Phys. Chem. Chem. Phys.* **2003**, *5*, 461; (b) Shynkar, V. V.; Klymchenko, A. S.; Piemont, E.; Demchenko, A. P.; Mely, Y. *J. Phys. Chem. A* **2004**, *108*, 8151; (c) Pivovarenko, V. G.; Wroblewska, A.; Błazejowski, J. *J. Mol. Struct.* **2004**, *708*, 175.
23. (a) Jung, H. S.; Kwon, P. S.; Lee, J. W.; Kim, J.; Hong, C. S.; Kim, J. W.; Yan, S.; Lee, J. Y.; Lee, J. H.; Joo, T.; Kim, J. S. *J. Am. Chem. Soc.* **2009**, *131*, 2008; (b) Ressalan, S.; Iyer, C. S. P. *J. Lumin.* **2005**, *111*, 121; (c) Choi, M.-Y.; Chan, M. C.-W.; Zhang, S.; Cheung, K.-K.; Che, C.-M.; Wong, K.-Y. *Organometallics* **1999**, *18*, 2074; (d) Villata, L. S.; Wolcan, E.; Feliz, M. R.; Capparelli, A. L. *J. Phys. Chem. A* **1999**, *103*, 5661.
24. Li, H.; Gao, S.; Xi, Z. *Inorg. Chem. Commun.* **2009**, *12*, 300.
25. Bush, A. I. *Curr. Opin. Chem. Biol.* **2000**, *4*, 184.
26. Lim, N. C.; Freake, H. C.; Bruckner, C. *Chem. Eur. J.* **2005**, *11*, 38.
27. Lu, C.; Xu, Z.; Cui, J.; Zhang, R.; Qian, X. *J. Org. Chem.* **2007**, *72*, 3554.
28. Xu, Z.; Yoon, J.; Spring, D. R. *Chem. Soc. Rev.* **2010**, *39*, 1996.
29. Thompson, R. B.; Jones, E. R. *Anal. Chem.* **1993**, *65*, 730.
30. (a) Koike, T.; Kimura, E.; Nakamura, I.; Hashimoto, Y.; Shiro, M. *J. Am. Chem. Soc.* **1992**, *114*, 7338; (b) Hartmann, U.; Vahrenkamp, H. *Inorg. Chem.* **1991**, *30*, 4676; (c) Elbaum, D.; Nair, S. K.; Patcham, M. W.; Thompson, R. B.; Christianson, D. W. *J. Am. Chem. Soc.* **1996**, *118*, 8381.
31. Denes, L.R. PCT Int. Appl., 1995, 78 pp. CODEN: PIXXD2 WO 9509846 A1 19950413 CAN 123:143917 AN 1995:723250 CAPLUS.
32. Keith, J. M.; Gomez, L. A.; Barbier, A. J.; Wilson, S. J.; Boggs, J. D.; Mazur, B. L.; Aluisio, C. L.; Lovenberg, T. W.; Carruthers, N. I. *Bioorg. Med. Chem. Lett.* **2007**, *17*, 4374.
33. Helal, A.; Kim, H.-S. *Tetrahedron* **2010**, *66*, 7097.
34. Velapoldi, R. A.; Tonnesen, H. H. *J. Fluoresc.* **2004**, *14*, 465.